

R E S E A R C H T R I A N G L E I N S T I T U T E

Second Quarterly Progress Report

December 27, 1983 through March 26, 1984

NIH Contract N01-NS-3-2356

Speech Processors for Auditory Prostheses

Prepared by

Blake S. Wilson and Charles C. Finley

Neuroscience Program Office

Research Triangle Institute

Research Triangle Park, NC 27709

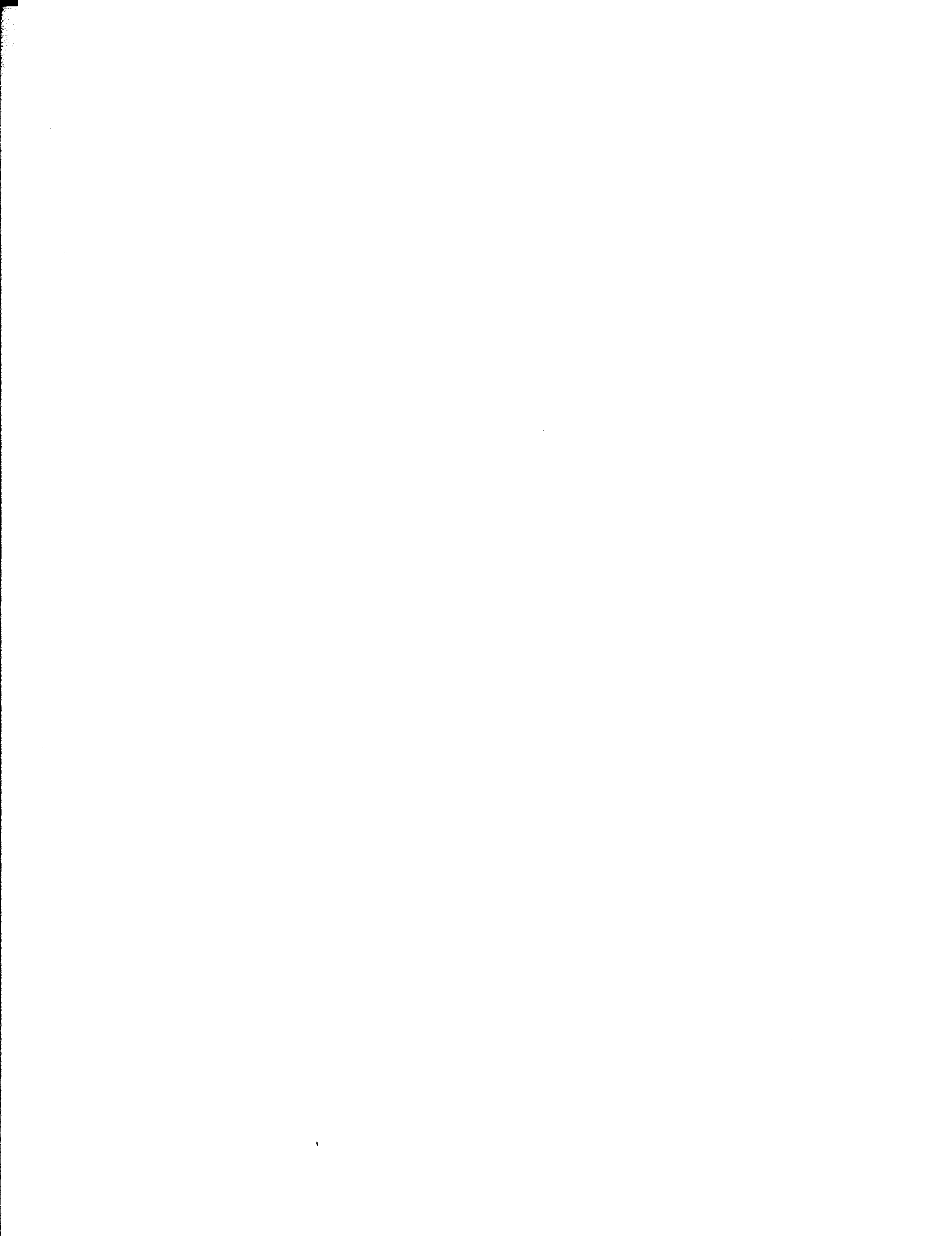
R E S E A R C H T R I A N G L E P A R K , N O R T H C A R O L I N A 2 7 7 0 9

ICPN = number of complex parameters for this function block;
CPARAM1 = complex parameter 1 of function block;

.

.

CPARAMN = complex parameter N of function block;
ICWORDS = complex array of dimension ICWORDS



CONTENTS

I.	Introduction	3
II.	Model of Field Patterns Produced by Intracochlear Electrodes	5
A.	Introduction	5
B.	Two-Dimensional Cross-Sectional Model	7
C.	Initial Results	9
D.	Future Modeling and Experimentation	12
E.	Future Significance of the Modeling Approach	13
F.	References	17
III.	Collaboration Between UCSF, Storz Instrument Co., RTI and Duke University Medical Center	25
IV.	Plans for the Next Quarter	27
Appendix 1: Description of the RTI Interface for Communication Between the Eclipse Computer and Patient Electrodes		29
Appendix 2: Notes on Software Development for the Block-Diagram Compiler		48

Introduction

The purpose of this project is to design and evaluate speech processors for multichannel auditory prostheses. Ideally, the processors will extract (or preserve) from conversational speech those parameters that are essential for intelligibility and then appropriately encode these parameters for electrical stimulation of the auditory nerve on a sector-by-sector basis. Work in this quarter was directed at (1) completing the design and beginning the construction of a hardware interface between an Eclipse computer and patient electrodes, for use in upcoming tests at the University of California at San Francisco (UCSF); (2) further development and near completion of the software for our computer-based simulator of multichannel speech processors, for use in the same tests; (3) development of a list of speech-processing strategies the RTI team would like to evaluate in these tests; (4) continuing our effort to form a productive collaboration between UCSF, Storz Instrument Company, RTI and the Duke University Medical Center (DUMC) for parallel evaluation of speech processors at UCSF and Duke; and (5) initial development of a finite-difference model of field patterns produced by intracochlear electrodes. In addition, our collaborators at UCSF have revised the software of the Klatt speech synthesizer so that it will run on the Eclipse computer and are now digitizing the "kernal" of the mini-MAC test (i.e., a subset of the Minimal Auditory Capabilities Battery designed by Elmer Owens and others) for use as inputs to our computer-based simulator of speech processors. In summary, then, we have accomplished all tasks outlined for this quarter in our last quarterly report and have initiated a new study to model the field patterns (and resulting patterns of neural excitation and block) produced by intracochlear electrodes. Preliminary findings of this last study indicate that the model, once fully

developed, will be extremely useful for evaluation and improved design of intracochlear electrode arrays, and for identification of optimal stimulus waveforms and stimulus paradigms to couple the outputs of speech processors to intracochlear electrodes. Because the modeling study is new, and because preliminary findings of this study are promising, the major part of this report will be devoted to its description. In addition, a complete description of the hardware interface for communication between the Eclipse computer and patient electrodes is presented in Appendix 1 and notes on software development for our computer-based simulator of speech processors are presented in Appendix 2. Finally, brief sections are included to indicate the present status of the collaboration between UCSF, Storz Instrument Company, RTI and Duke, and to outline our plans for the next quarter. Discussion of our list of speech-processing strategies is deferred until our colleagues at UCSF can review it and provide their suggestions for improvements.

Model of Field Patterns Produced by Intracochlear Electrodes

Introduction

It is clear that the success of advanced speech processor designs is largely dependent upon the success with which neural elements can be predictably and discretely stimulated. Knowledge of electrical stimulation phenomena has been largely sought along two avenues. One is the description of VIIIth nerve firing in electrically-stimulated animal cochleas. The other is psychophysical experimentation with implanted patients. Both approaches are empirical and will require extensive experimentation before a good appreciation of the mechanisms is achieved. With regard to the human experiments, it is unlikely that identification of an optimum electrode would ever be achieved given the relatively small number of implanted patients, the biological diversity due to differing neuron survival patterns, and the variety of experimental stimulation procedures used to drive the electrodes. This point is evident when one considers the broad range of electrode configurations used in laboratories around the world. Unfortunately, there does not appear to be a single body of knowledge available with which these various strategies may be objectively evaluated and compared, other than the current approach of comparing the overall success of each respective prosthesis system. Consequently, we have initiated an effort to construct a biologically-authentic computer model of the physical structures and biophysical mechanisms thought to be involved in transduction of electrical stimulation to neural cochlear outflow. Our plan is to describe as accurately as possible the biological and physical parameters involved (i.e., tissue and electrode impedances, electrode positions and orientations, and normal and pathological neural characteris-

tics) and then to study the relationships of these parameters as they impact upon the stimulation of and the dynamic performance of the surviving neural elements within the implanted cochlea. Ultimately, we hope to achieve the following:

1. an identification of the most significant and sensitive factors in the design of an implantable electrode array;
2. an identification of the behavior of the neural elements depending upon their spatial position relative to the stimulating electrodes;
3. an identification of the behavior of the neural elements depending upon the temporal and magnitude characteristics of the electrical stimulation waveforms;
4. an identification of the factors contributing to channel interactions with emphasis on finding ways to reduce and/or exploit such interactions;
5. an estimation of the spatial distribution and temporal firing characteristics of the population of neural elements stimulated by any given electrical stimulus delivered to selected electrodes in the array;
6. the application of the above knowledge toward the design of an electrode configuration that optimally meets the clinical objectives of the overall prosthesis design;
7. the application of the above knowledge toward optimizing the transfer of speech information from the speech processor to the central nervous system, by best simulating normal cochlear transduction.

The following subsections describe the overall experimental approach, initial results to date, plans for future experimentation, and thoughts on the ultimate applications of the model predictions.

Two-Dimensional Cross-Sectional Model

The model consists of an iterative two-dimensional finite element description of a cochlear cross section containing the three scalae, the spiral ganglion, and a bipolar electrode pair in the scala tympani. The electrode pair represents the current UCSF bipolar electrodes compressed into two dimensions. Grid points in the model are 20 microns apart and the two-dimensional sheet is assumed to be 20 microns thick. Presently, no assumptions are made relative to tissue characteristics in the planes parallel to the cross section, other than that complete symmetry exists. Potential distributions are computed by first defining a heterogenous resistive plane which describes the resistive characteristics of the various tissues seen in cross section. The electrodes, with their associated resistances, are described in this plane as well. Fixed potentials are defined for the electrode regions, and the perimeter of the cross-sectional grid is assumed to be a neutral ground with a potential level midway between the potentials of the electrodes. Calculations consist of treating each grid point in the plane as a resistive node, surrounded by four adjacent nodes. Current node equations are solved to compute a new grid-point potential. This process is iteratively executed until the total absolute potential change, summed across all grid points, is less than 5% of the interelectrode voltage. With the present grid size of 120 by 120 points, one iteration lasts about 35 seconds, using the hardware floating-point processor of our Data General Eclipse computer. Approximately 300 to 400 iterations are required to achieve the error criterion.

This model differs considerably from the lumped-element models which presently figure heavily in the cochlear prosthesis literature. The lumped-element models focus upon the space constants along each of the scalae and provide limited insight into the tradeoffs between close longitudinal spacing of electrodes (or electrode pairs) and channel interactions. These models are of no real use in the prediction of neural excitation due to electrical stimulation and fail to provide insight into the biophysical phenomena occurring in the immediate proximity of the stimulating electrodes themselves. Moreover, human experimentation with multichannel electrodes, placed according to the lumped-element model results for minimizing channel interactions, reveal considerable electrode channel interactions in some patients. These channel interactions depend upon both spatial and temporal parameters and may correlate with the survival patterns of spiral ganglion cell dendrites in each patient. These results suggest that a more useful modeling approach would be one that accounts for both the spatial distribution of currents in the cochlea as well as the biological characteristics of the neurons, which underlie the temporally-dependent behavior of the system. It is important to note that any model will be limited in its predictive accuracy, but may yet serve a useful purpose in providing insight into the explanation of observed phenomena and the design of new experiments and stimulus techniques.

The two-dimensional, finite-element model is most attractive in that it allows the calculation of complex field patterns which exist in heterogeneous structures of varying tissue types. For present purposes, the cochlear tissues are assumed to be purely resistive and isotropic. Anisotropic characteristics, which are known to exist in bone and myelinated nerve bundles, may be added later as the model is improved. The initial step in

the model description is the representation of the electrode array. Figure 1a shows the representation of a USCF bipolar electrode pair with a 90 degree interelectrode angle. The electrodes are assumed to be mounted in an insulator medium with the entire electrode assembly located in a homogenous resistive plane. Field potential patterns have been calculated assuming a fixed potential difference between the electrodes. The field distribution is indicated by equipotential contours (+ or - 1%) placed at 10% increments of the fixed electrode potentials. A current density diagram may be obtained by drawing contours perpendicular to the equipotential contours.

The purpose of the finite-element model is to describe the electrical nature of the cochlear tissues in cross section around the electrode. Figure 1b illustrates our plan for the final two-dimensional model. The cochlear cross section shown is a cartoon. Cross sections used for final calculations will accurately represent sections through actual cochleas at different turns. The anatomically-accurate cross sections will be entered into the computer by using a data tablet to digitize photographs of histological cross sections.

Initial Results

For the purpose of the present discussion, we assume that the field shown in Figures 1a and 1b approximates the actual field for the given cross section. This assumption will be tested when the anatomically-accurate cross sections are entered and fully modeled. The fields of ultimate interest are those which lie in the region of the myelinated spiral ganglion cells. Models of the response of myelinated neurons to electrical stimulation predict that sites of spike initiation occur where the maximum voltage gradients exist between adjacent nodes of Ranvier. Disregarding polarity considerations, it is evident that for the neuron shown in Figure 1b, the

initiated spike would begin in the dendrite region where the voltage gradients are the steepest, as opposed to the more proximal axon which lies approximately tangent to the equipotential contours. To obtain further insight into the nature of the voltage gradient, Figure 1c shows an inset which represents the calculated voltage gradients along a straight line drawn along the approximate course of the neuron. The y-axis range of the inset is equal to the potential difference between the two electrodes. Points A, B, C and D indicate positions along the neuronal axis. The potential gradients along the neuron, as shown in the inset, are the greatest between points B and C, indicating the predicted region of spike initiation. Although the conclusions of the model are obvious here, field patterns obtained with anatomically-accurate cross sections are expected to be different. In addition, the question arises as to whether or not other electrode sizes, positions, and/or impedances will have significant impact on the field patterns.

As an illustration of our initial exploration of these latter issues, Figure 2b shows the field calculations of the same conditions of Figure 1 (repeated in Figure 2a), with the electrodes modeled as point sources instead of the previous button-shaped elements. These conditions, for Figure 2b, are those normally assumed for a bipolar electrode pair modeled as an electrical dipole. Comparing Figures 2a and 2b, it is clear that the field patterns are quite different and in particular that the potential gradients are steeper in the vicinity of the neuron when stimulation is with the button-shaped electrodes. This indicates that there are significant near-field patterns around the actual bipolar electrodes that alter the potential gradients around the target neurons. Therefore, the assumption that the bipolar electrodes behave as an electrical dipole appears to be unfounded.

Monopolar stimulation of the cochlea may be also modeled as shown in Figures 3b and 3c. Figure 3b shows the field pattern when the upper-most electrode (black) is driven relative to a remote ground return electrode. The remaining electrode in the scala tympani is allowed to float. Figure 3c shows the field patterns when the lower-most electrode is driven in a similar monopolar fashion. Figure 3a repeats the previously-discussed bipolar field patterns for reference. It is evident from these fields that monopolar stimulation is far reaching in effect, resulting in greatly reduced specificity of stimulation. Comparing the results shown in Figures 3b and 3c indicates that significantly different stimulation results may arise depending upon which of the electrodes of the bipolar pair is driven in a monopolar fashion. For the same monopolar stimulus levels, the potential gradients along the neuron are much greater when the upper-most electrode is driven, Figure 3b. Significant current spread is a widely accepted notion in the cochlear prosthesis literature, yet the practice of monopolar stimulation is still widely used. With the model of monopolar stimulation, we hope to better evaluate the mechanisms active in other prosthesis designs.

As further demonstration of the ability to manipulate experimental parameters, Figures 4a, 4b and 4c show the field changes due to increasing the interelectrode angle from 90 degrees to 180 degrees for the bipolar pair. Note that the potential gradients along the neuron diminish as the angle increases. The 180 degree configuration approximates the Hochmair electrode used by the Austrian team. Figures 5a and 5b show the changes due to rotating the orientation of the UCSF electrode 45 degrees toward the spiral ganglion. The gradient diminishes slightly, but its position shifts toward the ganglion. This may be significant in cases of poor neuron survival. Figures 6a, 6b, 6c and 6d indicate the effects produced by

changing the position of the bipolar electrodes within scala tympani. Based on these results, electrode position within the scala is a significant design parameter (i.e., there are large differences in the field gradients, particularly for the conditions shown in panels 6c and 6d). Finally, Figures 7a and 7b depict the alterations in field patterns produced by reducing the bipolar electrode sizes and placing them closer together. The resultant field patterns are sharper and more circumscribed. Further discussion of the observed effects of these parametric changes is not warranted at present in that these calculations are only initial trial computations.

Future Modeling and Experimentation

The calculations of field distributions only provide a measure of the relative potential levels along the course of a spiral ganglion cell and its processes. Further calculations of action potential dynamics will be made by feeding the respective voltages of each node of Ranvier into a lumped-element model of a myelinated axon. McNeal's (1976) axon model, which consists of resistively linked Frankenhauser-Huxley nodes, will be used as a basic model. Two modifications will eventually be incorporated. One is the inclusion of lossy cable properties linking the F-H nodes instead of the purely resistive node interconnections of the McNeal model. This will enable accurate calculation of propagating action potentials. The other modification will be the description of the extra cellular node voltages as current sources in series with the extra cellular resistance. This will allow the node voltages to vary during calculated spike propagation. As a short note on the potential validity of the use of a mathematical neuronal model, it should be mentioned that this literature stems from the original Hodgkin-Huxley equations describing the giant squid axon. This original

work, and its many extensions, stand as one of the most remarkable successes in the modeling of a biological system. There is extensive work showing that these models accurately predict neuronal behavior in vivo.

A variety of possible electrode effects will be explored with the integrated field-neuron model, in addition to those already mentioned. In particular, the possibility arises that the relatively large button-shaped electrodes (see Figure 2) may exert substantial local (or near-field) effects on portions of a neuron, even though the two electrodes are being driven in a bipolar manner. Possibly, the effects of "anodal block" and/or "anodal break" may play a role during stimulation. These effects may effectively give rise to multiple generator sites as well as to blockage of cathodically-generated spikes. In addition, the temporal dynamics of the absolute refractory period, the relatively refractory period and accommodation phenomena further complicate the picture, but all can be computationally dealt with and evaluated in the model.

Validation of the model is of crucial importance to its ultimate utility. Clearly, one validation approach is to attempt to predict the results of numerous animal studies of VIIIth nerve responses to intracochlear stimulation. This will be clearly the most robust validation approach. Present expectations are that this validation will be straightforward. If the model proves effective here, then application of the model to the human cochlea is warranted. Michael Merzenich, during a recent visit to RTI, agreed to conduct animal and human experiments in his laboratories at UCSF to further test the model and/or its predictions, should circumstances warrant it.

Future Significance of the Modeling Approach

To summarize, the value of the two-dimensional model is largely focused on the following questions :

1. What are the relative effects of the heterogenous structure of the cochlea on the local field patterns in the vicinity of the spiral ganglion cells?
2. What are the optimal electrode configurations for intracochlear electrodes which discretely stimulate a limited population of cells?
3. What are the temporal ^{activation} ~~stimulation~~ characteristics of the neural elements in these electrode fields?
4. How do these characteristics limit speech-encoding strategies?

The greater issue of channel interactions is not directly addressed by the two-dimensional model. However, insight into the behavior of neurons local to a stimulating electrode pair will be essential toward understanding the factors controlling channel interactions. Finally, a three-dimensional model will yield the greatest insight into the channel interaction problem. The present two-dimensional iterative model can be expanded to three dimensions at great computational expense. Possibly, simplifying assumptions from the two-dimensional modeling, in particular that the cochlear tissue resistivities affect the actual field patterns only slightly, will reduce the simulation of the three-dimensional case to a relatively simple computation of linear summations at a point. If these simplifying assumptions are shown to be valid, only one three-dimensional computation of a single electrode pair would be required. Further discussion of the development of a three-dimensional model is deferred until complete results from the two-dimensional model are available.

Regarding the topic of channel interactions, several points may be made at this time.

(1) Judging from the presently limited two-dimensional model results, it is probable that the most significant channel interactions occur within the spiral ganglion itself. This hypothesis may be tested in at least two independent ways. One is to continue the modeling of potential fields to determine the loci of maximal summation of the field patterns of interacting channels. The experimental data useful in this approach are the "electrical" or spatial interactions obtained with synchronous channel stimulation. The other experimental approach is to carefully evaluate the temporal characteristics of channel interactions. A number of temporally-dependent mechanisms may underlie channel interactions. One is the strength-duration characteristic of a neuron. The details of how this factor affects channel interactions requires further thought, but it will undoubtedly be a significant factor in determining the optimum stimulation sequence for the encoding algorithm of the speech processor. A second temporal interaction between channels could arise from antidromically propagating spikes initiated by a basally located electrode pair (channel B), which collide with orthodromically propagating spikes initiated by a more apically located electrode pair (channel A). Possibly, a simple method of determining if these collisions occur would be to record the response measures (i.e. brainstem evoked responses and/or psychophysical reports; see also (2) below) to temporally delayed stimulations from channels A and B. If the responses to channel A followed by channel B are equal to the responses of channel B followed by channel A, there is little chance that significant spike collisions are occurring. It is difficult to say at this time how these possible effects may relate to the loudness-summation measures of channel interactions using comparisons of 0 degree and 180 degree phase conditions of two continuously stimulated channels (Shannon, 1984 preprint).

(2) Relative to the issue of measuring channel interactions, two methods are presently used in monitoring responses to stimulation in the human. These are the brainstem evoked response and the reporting of percepts by the patient. It appears that both of these measures may be biased when using the results to make inferences about the intracochlear mechanisms mediating channel interactions. Both techniques involve substantial processing of the activity of the VIIIth nerve before a quantifiable response is produced. As an alternative, we propose to simply record an "intracochlear" evoked response from a free pair of bipolar electrodes. This approach will provide a more direct measure of the specific gross activity of the spiral ganglion. This information may also be available at a higher signal-to-noise ratio, allowing reduced averaging and test time. Because these data may be less ambiguous and perhaps more may be collected in a given period, a more complete characterization of the channel interactions may be obtained. Interpretation these data in light of the modeling results could produce a physiologically-based model of how the prosthesis interfaces to the nervous system. Combining this knowledge with the information output from advanced speech processors, could, in turn, provide a basis for optimizing the stimulation strategy. Unique strategies, optimized for individual patients, may also be possible.

The RTI patient interface is being configured for this capability. In particular, electrical artifact rejection circuits are being included in the programmable ADC for monitoring channel activity.

References

McNeal, D. R., Analysis of a model of excitation of myelinated nerve,
IEEE Trans. Biomed. Eng., 23 (1976) 329-337.

Shannon, R. V., Loudness summation as a measure of channel interaction in a
cochlear prosthesis, 1984 preprint.

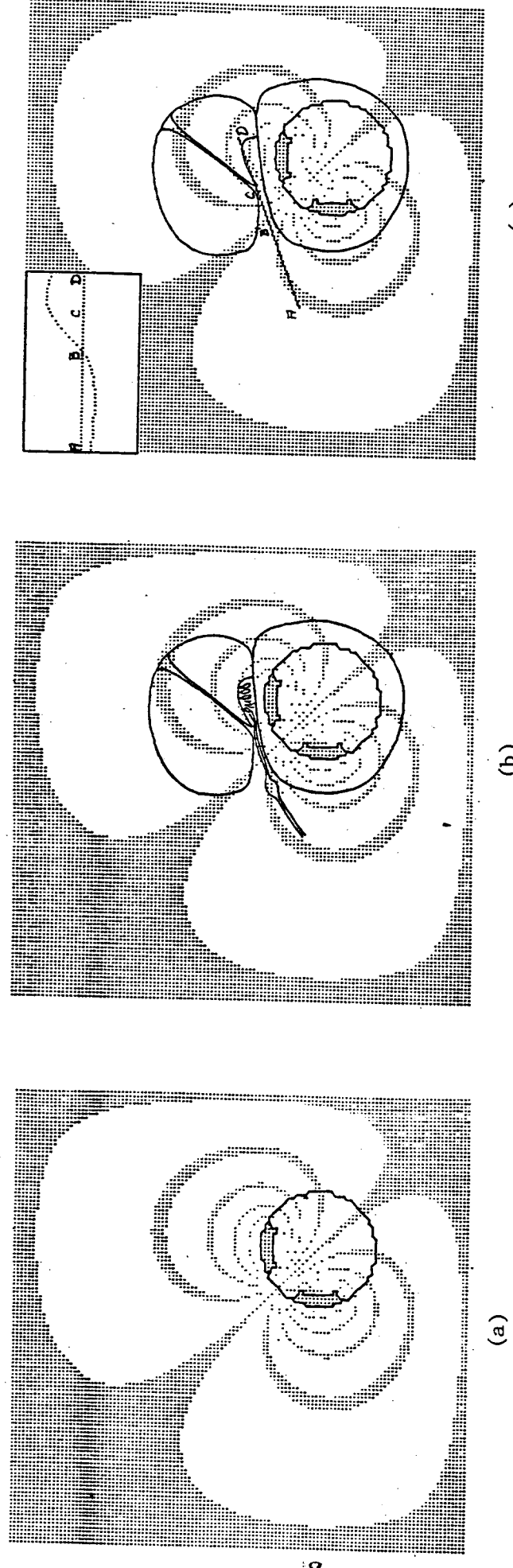
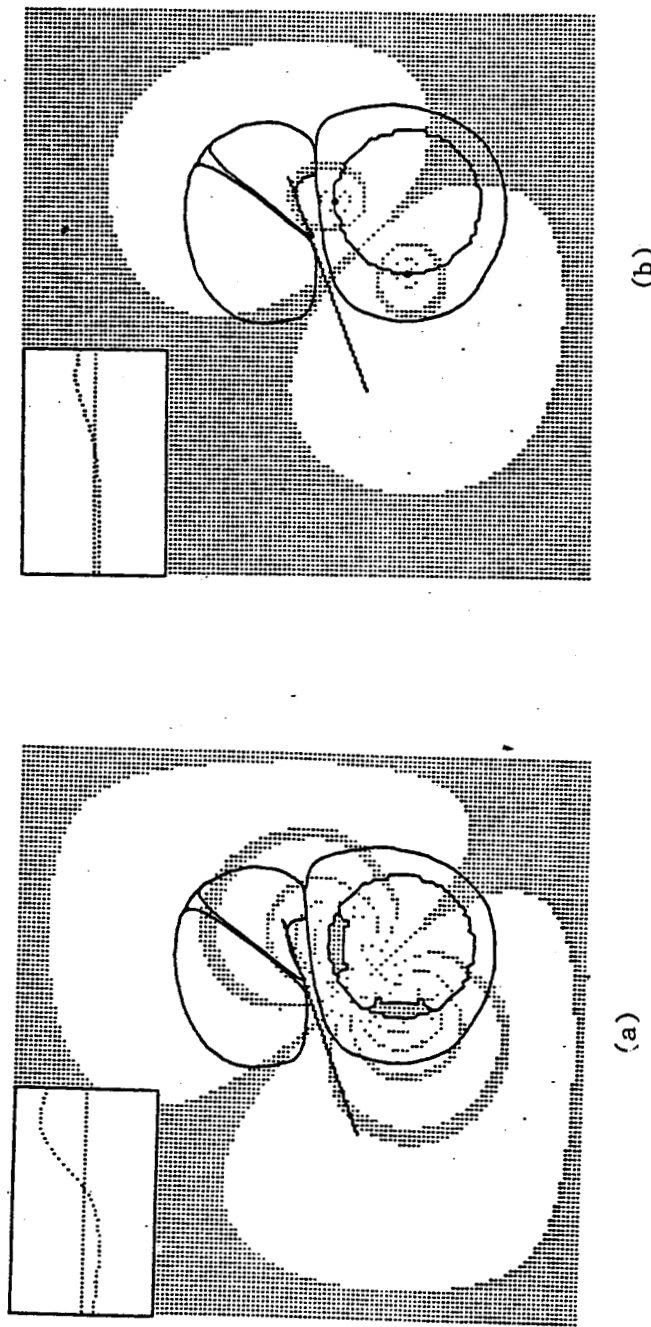
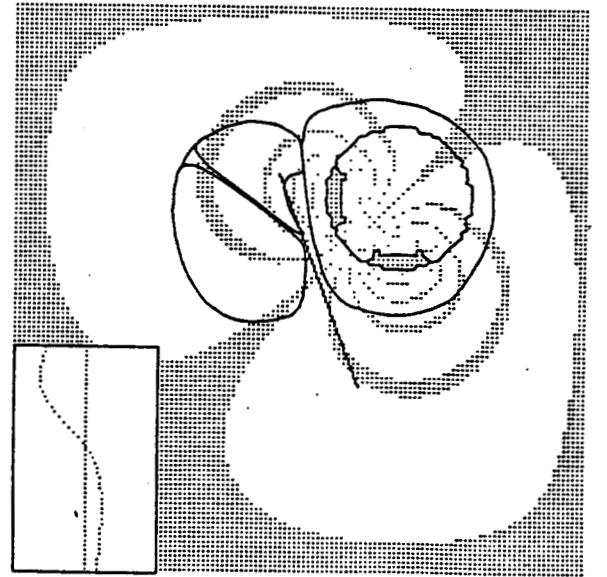


Figure 1. Description of two-dimensional finite-element model.

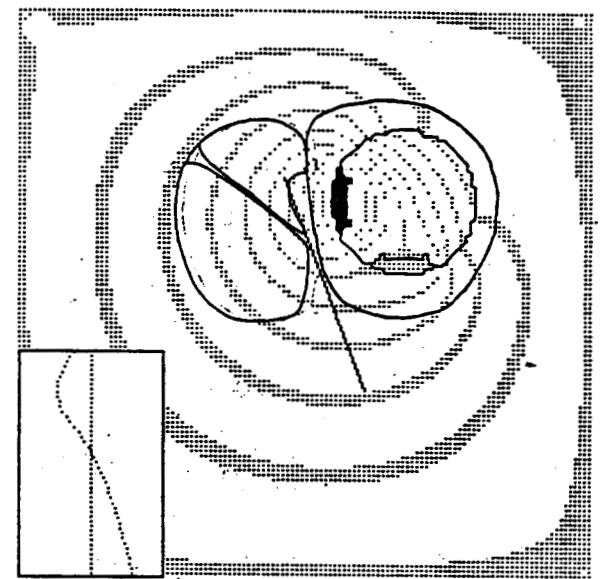
- (a) UCSF bipolar electrode pair and computed field pattern
- (b) Electrode and field pattern with overlay of cochlear cross section
- (c) Same as (b) but with inset showing potential levels along neuron (see text)

Figure 2. Field patterns for an actual bipolar pair (a) and a true dipole (b) configuration.

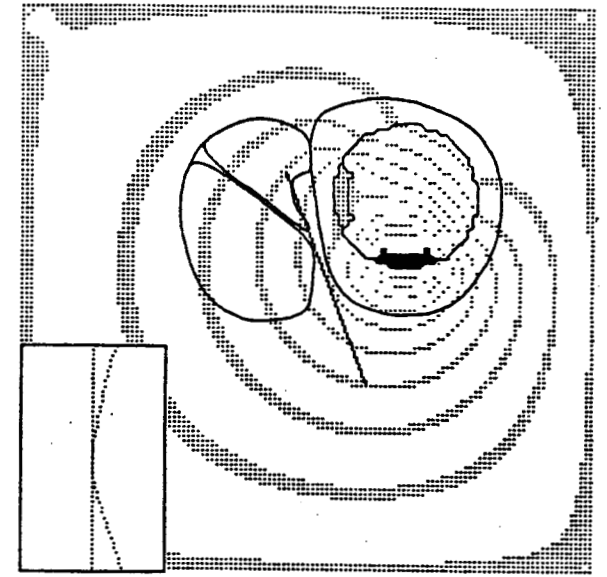




(a)



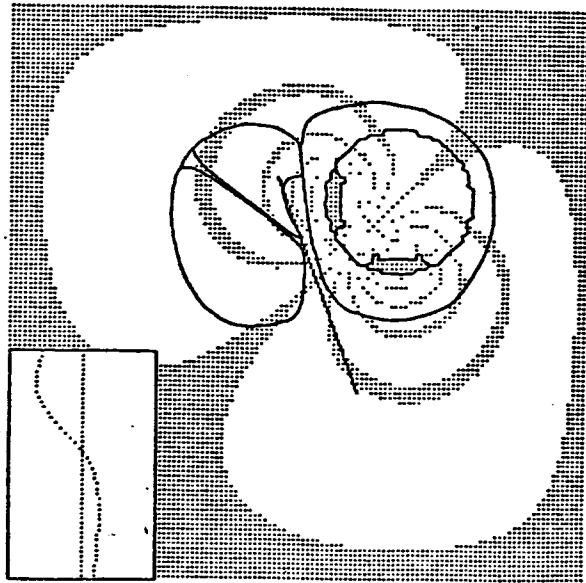
(b)



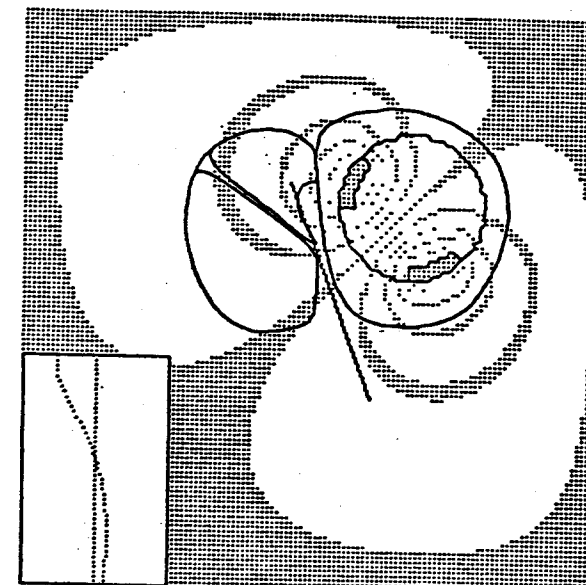
(c)

Figure 3. Field patterns for standard bipolar (a) and monopolar (b and c) configurations.

(a)



(b)



(c)

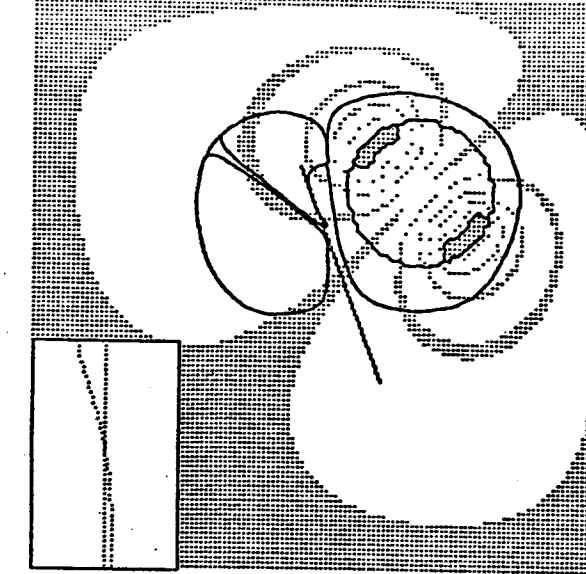
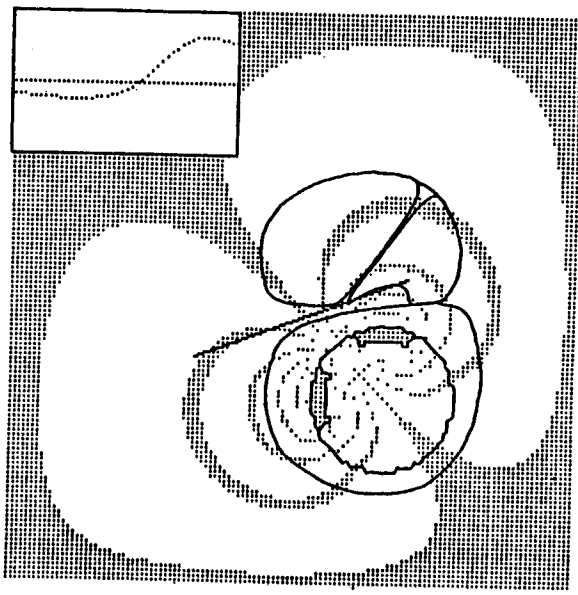
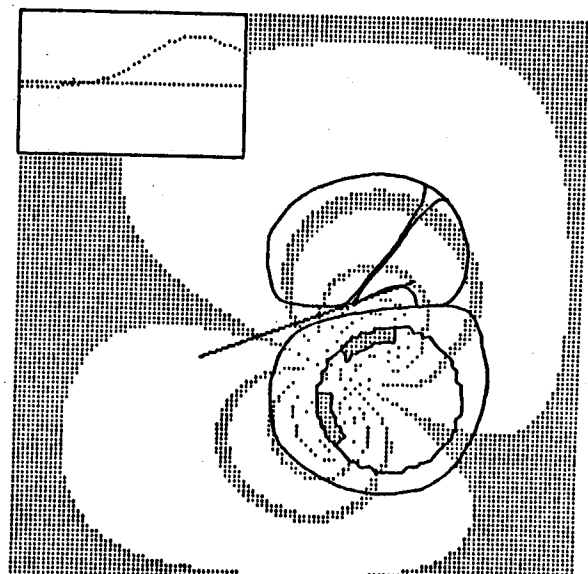


Figure 4. Field patterns for bipolar electrodes configured with differing interelectrode angles of 90° (a), 135° (b), and 180° (c).



(a)



(b)

Figure 5. Field patterns for standard bipolar electrodes configured with different rotational positions of 0° (a) and 45° (b) toward the spiral ganglion.

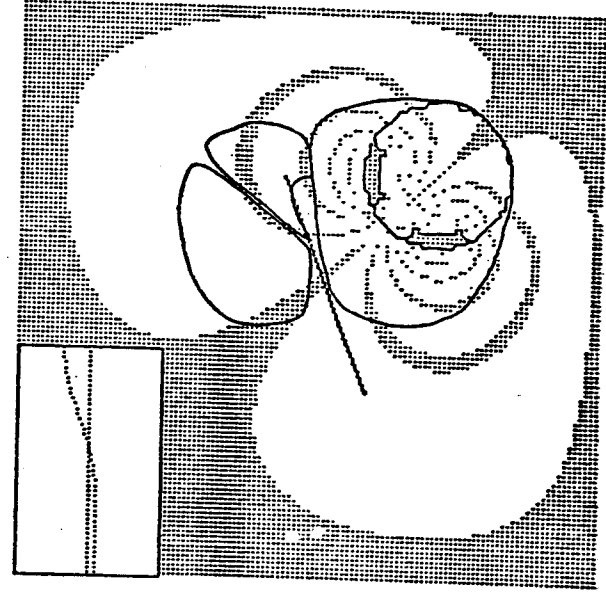
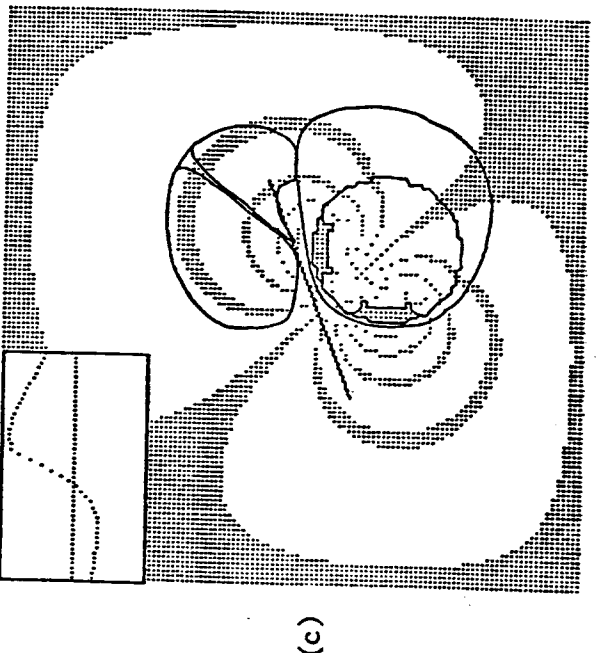
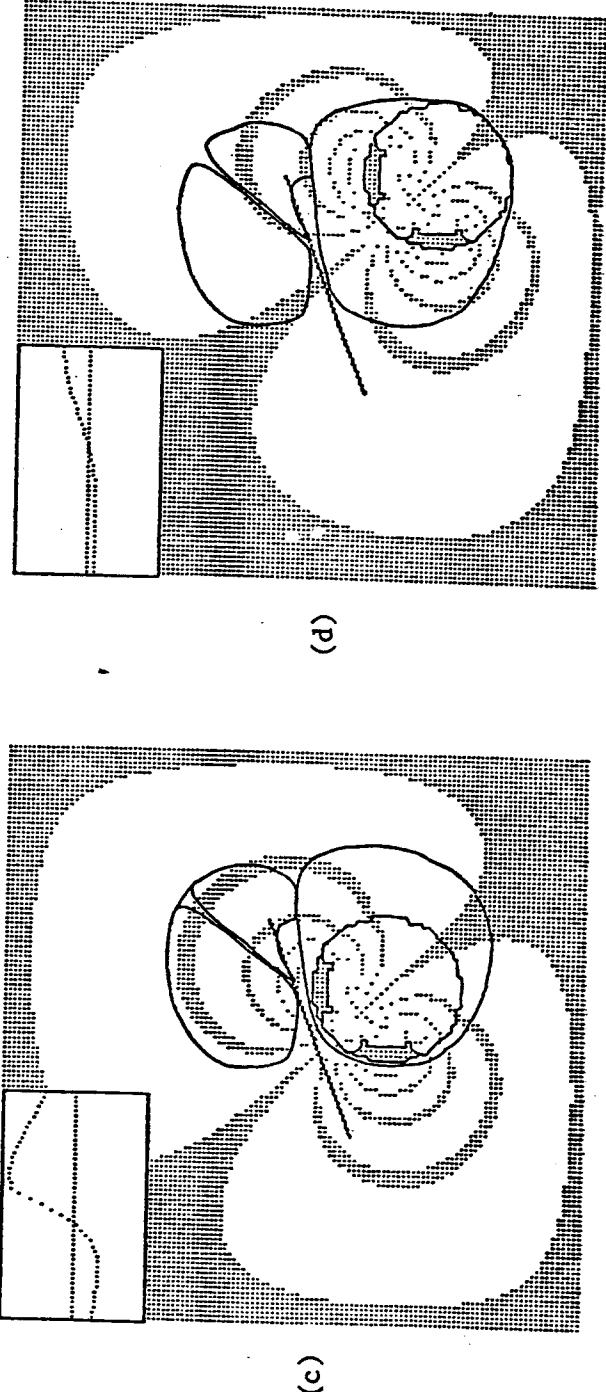
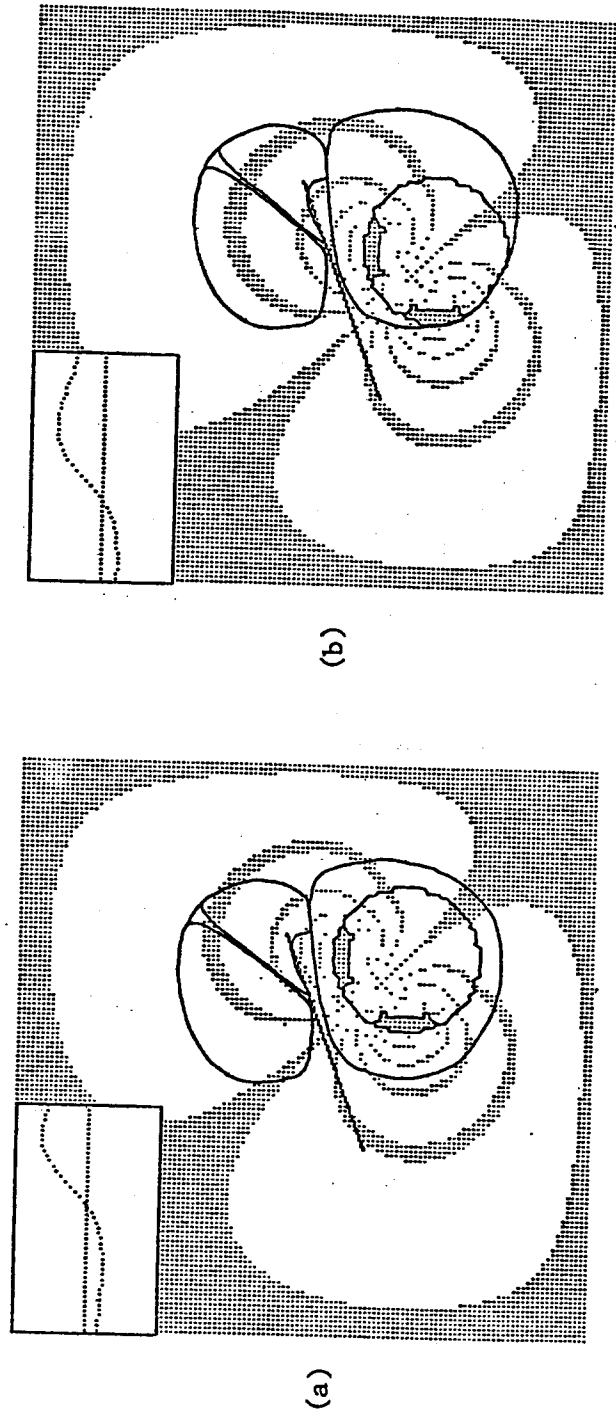
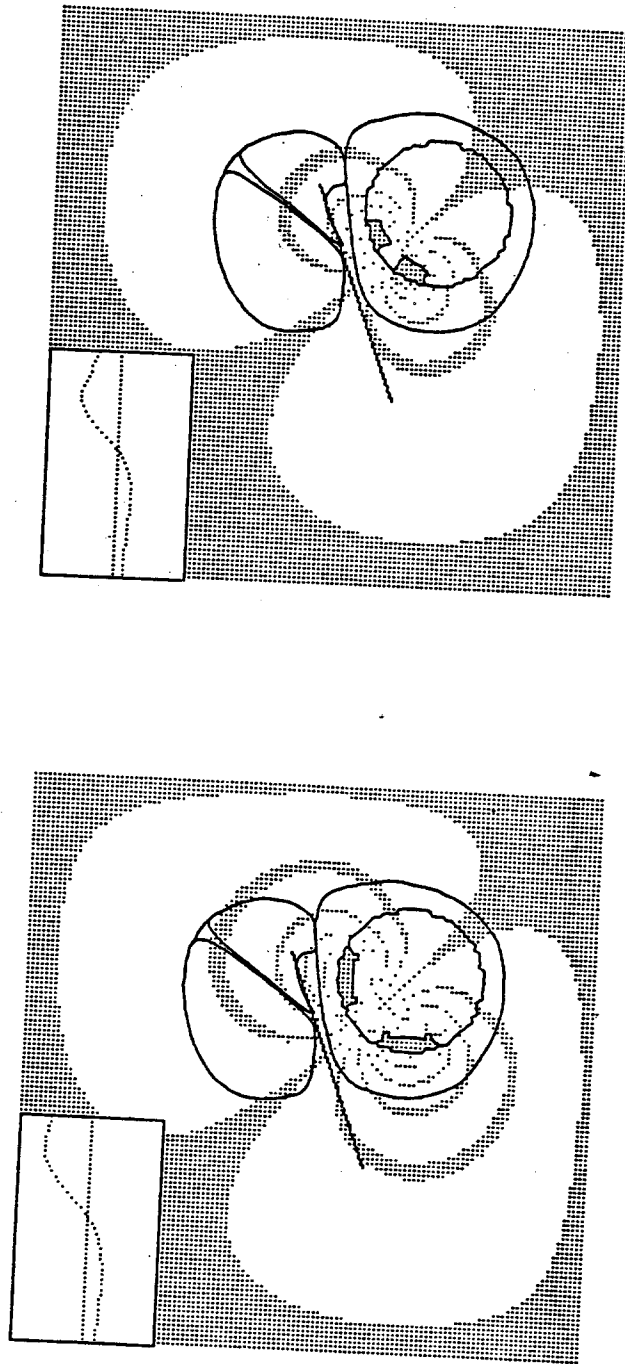


Figure 6. Field patterns for the standard bipolar pair located at different positions within scala tympani.

Figure 7. Field patterns for the standard bipolar pair (a) as compared to a smaller and more closely spaced bipolar pair (b).



Collaboration Between UCSF, Storz Instrument Company, RTI and DUMC

Mike Merzenich and two representatives from Storz Instrument Company, Dave Calvert and Steve Hutchison, visited RTI and Duke on March 21 to discuss Duke's potential participation as an "experimental collaborator" in UCSF's program to develop the next generation of multichannel auditory prostheses. Dr. Merzenich outlined the present status of the four-channel UCSF prosthesis to the group at Duke and described the plans UCSF and Storz have for experimental and clinical collaborators. The suggestion was made that Duke participate as both, and that all four parties work closely together to conduct parallel tests at UCSF and Duke for evaluation of speech-processing strategies for multichannel prostheses. This suggestion was adopted by the group and preliminary arrangements have been made to start in earnest the new program at Duke. We expect that surgeons and audiologists from the Duke team will travel to San Francisco in the next month or two for training on the implant procedure and on evaluation and rehabilitation of patients. We hope that our first implant at Duke will be performed this Fall. A percutaneous connector will be used for this and subsequent patients. This connector will provide direct access to all electrodes in the implanted array so that we can duplicate at Duke the computer-based tests of speech-processing strategies we will be conducting at UCSF. If funds can be identified to support various aspects of the experimental tests at Duke, then the number of patients included in the present project could be approximately doubled. Additional support is required for the following: (1) installation and upgrading of a "spare" RTI Eclipse computer at Duke; (2) construction of an additional interface between the Eclipse and patient electrodes, for use at Duke; (3) computer supplies and maintenance associated with the conduct of tests at Duke; (4)

the time of RTI personnel who will help design and execute the tests at Duke; (5) upgrading the facilities for audiological evaluations at Duke so that speech perception by cochlear-implant patients can be fully measured; and (6) the time of Duke personnel not supported by third-party payments. We are seeking support for the activities and supplies just listed from the NIH (through the grants route, with a joint application from UCSF, RTI and Duke), Storz Instrument Company and the Burroughs Wellcome Fund. In addition, we have requested a small amount of "start-up" money from limited funds available to Duke's Department of Surgery for such a purpose. Because the potential benefits of parallel tests at Duke to the present project are many, we would also like to request supplemental funding from the Neural Prostheses Program to support some or all of RTI's participation in the program at Duke. We will continue to keep the technical monitor of the present project fully informed of all developments (funding and otherwise) related to our new program at Duke.

Plans for the Next Quarter

Our plans for the next quarter are centered around the preparation and conduct of tests at UCSF to evaluate speech-processing strategies for multi-channel auditory prostheses. Two patients will be tested; one was implanted on March 13 and the other will be implanted within the next one or two months. To prepare for these tests, RTI personnel must complete construction and checkout of the hardware interface between the Eclipse computer and patient electrodes, and must complete the software for the computer-based simulator of speech processors. As indicated in the two appendices of this report, we are well on our way to accomplishing both. These tasks will have high priority in the first few weeks of this quarter. Once completed, we expect to spend between 2 and 4 weeks in San Francisco to work with the UCSF team in evaluating speech-processing strategies. The list of strategies to be evaluated will be jointly composed by investigators on the RTI and UCSF teams. As indicated in the Introduction, an initial "straw-man" list composed by the RTI team has been sent to UCSF for review and comments. We expect to have the final list completed over the next three or four weeks, in time to guide our tests with the patient implanted on March 13 (a three-month period is allowed for psychophysical testing of patients in the experimental series, after which the percutaneous connector is removed and the internal connector pad configured for use with the four-channel rf link of the portable processor). Thus, in the next quarter we plan to meet or exceed all of the original objectives for the first year of this project (to "design and implement a computer-based, multichannel auditory signal processor for use in evaluating promising speech extraction and stimulus encoding schemes"). In addition, we plan to begin testing of implanted patients at UCSF, which is a new objective recently approved by the

technical monitor and contracting officer for this project. Now that the tools for design and evaluation of speech processors for multichannel auditory prostheses are nearly complete, we are anxious to put them to the best-possible use in collaboration with our talented colleagues at UCSF.

Appendix 1

Description of the RTI Interface for Communication Between the Eclipse Computer and Patient Electrodes

Contents:

RTI Patient Interface Description	30
Patient Safety Design Features	31
Data General Hardware Requirements	32
Patient Interface Software Control	33
Patient Connection	36
Patient Disconnection	36
Channel Magnitude Control	37
Patient Channel Electrode Voltage Monitoring	40
Impedance Monitoring	41
Automated Functional Checkout Routines	42
Patient Electrode Connection and Selection	43
Circuit Diagrams	45

RTI PATIENT INTERFACE DESCRIPTION

The RTI Patient Interface is essentially a redesign of the existing UCSF Interface described in Mark White's thesis, Chapter 5. A redesign was initiated to take advantage of newer technology and to provide expanded system flexibility. The basic UCSF design features of stimulus charge limiting and patient safety precautions have been retained in the RTI design. The most significant design features include:

- a total of eight patient channels, each consisting of a computer controlled-stimulator for a bipolar electrode pair;
- independent channel functions with electrically floating grounds and isolated supplies;
- synchronization of all stimulus channel magnitude transitions with 50 usec. temporal resolution;
- integrated DAC's in the circuitry of each patient channel;
- optical isolation using a linear optically-driven FET thus reducing circuit complexity;
- continual monitoring of electrode voltages across any program-selected channel with an onboard ADC;
- electrode impedance measurement capability under program control between any two patient electrodes;
- patient connection or disconnection to or from the interface under program control;
- modular packaging of circuitry for each patient channel in a Vector Electronics plug-in module with all eight patient channels occupying a 5 1/2 inch high standard rack panel (Power supplies are additional).

PATIENT SAFETY DESIGN FEATURES

Patient safety design features parallel the UCSF design and are listed here for review:

- optical isolation of analog circuitry;
- dual output blocking capacitors of low capacitance and low leakage;
- series current limiting resistors in patient leads;
- 2 mA patient lead fuses;
- patient disconnect relays on each channel operating under patient control or with an automatic timeout period of 50 usec;
- current limiting (2 mA) of both positive and negative drives of output op-amps.

The last item is a new design feature drawing on currently available high voltage op-amps with current limiting options.

The present RTI design does not incorporate the UCSF feature of a variable voltage battery supply. Instead, the high voltage supply for each patient channel consists of a standard "brick" supply, driven with an isolation transformer. This choice was made for the long term convenience of reduced maintenance and to avoid continued operating costs for battery replacement.

DG INTERFACE HARDWARE REQUIREMENTS

The Patient Interface communicates with the DG Eclipse system using the I/O capabilities of the DG Digital Control Unit, Model 50 (DCU/50). The DCU/200 may also be used. The DCU/50 is a user-programmable processor with 1024 words of onboard ROM and is capable of sharing 31,744 words of memory with the Eclipse via data channel communications. The DCU/50 essentially handles fast I/O between the Eclipse data bus and the DCU/50's own data bus. The DCU/50 communicates with the Patient Interface via a 16 bit parallel I/O interface (DG 4066), which resides on the DCU/50 data bus. Patient channel data rates are sufficient to provide a channel frequency response of 20 kHz.

DG hardware requirements for Patient Interface control include:

- one DCU/50 or DCU/200 I/O processor
- one 4066 parallel I/O interface
- one 4251 communications chassis for DCU data bus.

PATIENT INTERFACE SOFTWARE CONTROL

In general, the programmer has the capability to :

- (1) connect or disconnect the patient to or from the stimulation system;
- (2) on a channel-by-channel basis selectively change the stimulus magnitude every 50 usec if desired, otherwise the previous magnitude value is maintained;
- (3) continually monitor the voltage across the electrode pair of a program-selected patient channel;
- (4) monitor impedance between any two program-selected patient electrodes;
- (5) perform automatic functional testing and calibration verification;
- (6) enable or disable the 50 usec. clock onboard the interface, which times the DAC output conversions for all patient channels;
- (7) reset the Synchronization Error Flag after an error has been signalled from the interface;
- (8) determine identification number of the currently installed Electrode Selection Jumper Plug.

Operation of the Patient Interface with regard to each of these capabilities is detailed in the following paragraphs.

Program control of the Patient Interface is accomplished by passing 16-bit words via the DG 4066 parallel I/O interface. Each word consists of a 4-bit (most significant nibble) command field and a 12-bit data/function field. The 4-bit commands are summarized below.

CONTROL WORD (hex)	FUNCTIONAL DESCRIPTION
0***	Latch current data value (**) to patient chan 0
1***	" " " " " " " " " " " " " " 1
2***	" " " " " " " " " " " " " " 2
3***	" " " " " " " " " " " " " " 3
4***	" " " " " " " " " " " " " " 4
5***	" " " " " " " " " " " " " " 5
6***	" " " " " " " " " " " " " " 6
7***	" " " " " " " " " " " " " " 7
8XXX	End Of Command String (EOC)
9GPN	Configure ADC Connections
AXXI	Impedance Testing Mode Control
BXXX	Enable Interrogation Of Electrode Jumper Plug Number
CXXJ	50 usec. Interface Clock Control
DXXX	DCU/Interface Synchronization Error Flag Reset
EXXX	Connect Patient
FXXX	ABORT RESET ! - Disconnect Patient

Where

*** is current 12-bit data word (one's complement)

G is patient channel number for ADC Ground connection

P is electrode number for ADC Positive input connection

N is electrode number for ADC Negative input connection

I is control value for Impedance Testing Mode

if I = 0, exit Impedance Testing Mode

if I = 1, enter Impedance Testing Mode

J is control value for Interface 50 usec. Clock

if J = 0, disable clock

if J = 1, enable clock

K is control value for interrogation of identification number of the
currently installed electrode selection jumper plug

if K = 0, disable this mode

if K = 1, bits 12 - 15 of input word to parallel interface
contain the jumper number

X don't care.

Patient Connection -

Control Word: EXXX

Function: Sets flag PC, which enables the capability of End Of Command (EOC) instructions to reset timing cycle of patient disconnect relay driver.

Patient connection continues only as long as command strings terminated by EOC are being actively sent to the interface every 50 usec.

CAUTION: All patient output channels should be zeroed prior to execution of this instruction.

Patient Disconnection -

Control Word: FXXX

Function: Set flag PD, which forces an immediate interface reset thus disconnecting the patient from the stimulation system. An automatic patient disconnect occurs if the timeout disconnect period timer has not been reset within the current 50 usec. interval by the EOC command.

Channel Magnitude Control -

Control Words: #***, #***, #***, , #***, BXXX

where # is patient channel number (0-7)

*** is 12-bit one's complement data value for DAC

BXXX is the End Of Command (EOC) control instruction.

Function: This instruction string transfers stimulus output magnitude values to each patient channel specified in the control word. These stimulus magnitude values are stored in data latches for each channel as the control word is received. The latched magnitudes are then transferred to the channel DAC's at the beginning of each 50 usec. period, thus providing synchronization across all channels. If a stimulus magnitude value is not sent to a particular channel, then the previous latch value is retained for transfer to the DAC again. Consequently, presentation of a stimulus series requires only coding of changes of stimulus magnitude. Sustained values across one or more 50 usec. periods are automatically retained.

The EOC command must terminate the transmission of stimulus magnitudes for every 50 usec. period. The EOC command performs several functions:

(1) the EOC allows a synchronization check between the Eclipse data transmission and the 50 usec. interface clock to ensure that all patient channel stimulus level updates have been received prior to the beginning of the next 50 usec. period. In the event that an EOC has not been received in time, the patient is automatically disconnected and an interrupt with the synchronization error flag set is issued to the Eclipse;

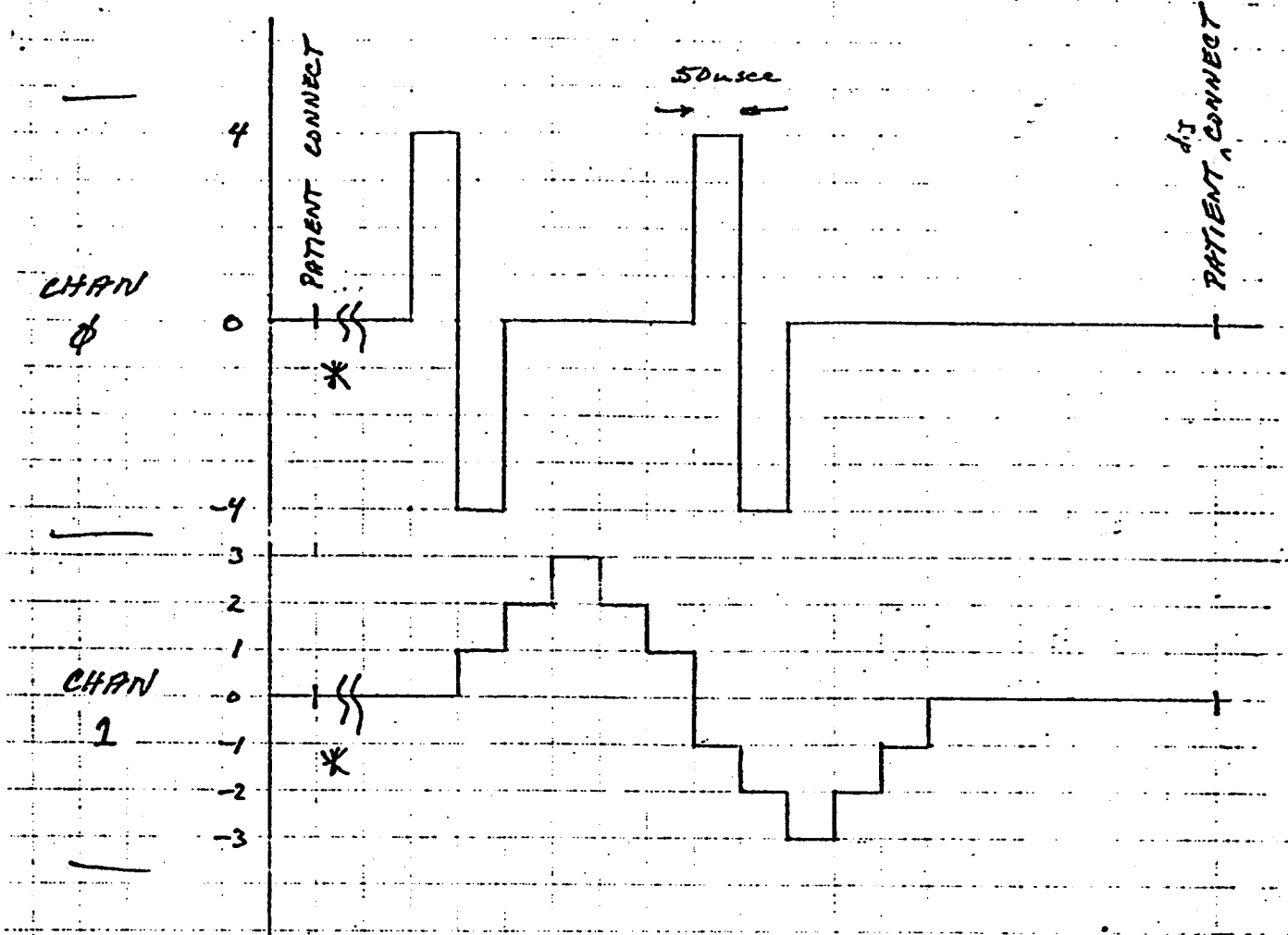
(2) the EOC occurrence every 50 usec. serves as an indicator of a flow of stimulus commands from the DCU, thus keeping the patient connected to the system. Should the data flow be interrupted, as indicated by an EOC not being received within a 50 usec. period, the patient is automatically disconnected. This latter state is flagged as a synchronization error, as

in (1) above;

(3) the EOC, by itself, indicates a 50 usec. stimulus magnitude coding periods during which no patient channel stimulus levels are modified. Stimulus delays to allow for relay contact bounce, while still maintaining patient connection, are achieved by a continuous string of EOC's. Twenty (20) EOC's, one every 50 usec., give a 1 msec. delay.

NOTE: As a possible way to condense stimulus code storage, the EOC command format for disc storage may be changed from 8XXX to 8%%, where %% is the number of consecutive EOC's to output before progressing. As such, a 10 usec. delay (200 EOC's) could be coded simply as 80C8 (hex). This feature will require additional processing demands on the DCU service routine; however, present indications are that the final implementation will have this capability.

The following page illustrates the stimulus coding required to output two different stimulus sequences simultaneously on two different channels. The Channel 0 output is a 50 usec. biphasic spike train, whereas the Channel 1 output mimics a continuously variable analog signal.



The command string to output this stimulus sequence would be:

(START)	CH0, 0	CH1, 1	EDC
	CH1, 0	EDC	EDC
	EDC	CH0, 4	EDC
		EDC	EDC
		CH1, -1	EDC
PATIENT CONNECT COMMAND		EDC	EDC
400 EDC's in delay for segment delay	EDC	CH0, -4	EDC
bounce	CH0, 4	CH1, -2	PATIENT DISCONNECT COMM
	EDC	EDC	(END)
	CH0, -4	CH0, 0	
	CH1, 2	CH1, -3	
	EDC	EDC	
	CH0, 0	EDC	
	CH1, 2	CH1, -2	
	EDC	EDC	
	CH1, 3	CH1, -1	
	EDC	EDC	
	CH1, 2	CH1, 0	
	EDC	EDC	
cont			

* // indicates an interval in which a string of repeated EDC's, one every 50usec are required for a time delay during which patient disconnection logic occurs (approx 20 msec)

Patient Channel Electrode Voltage Monitoring -

Control Word: 9GPN

where G is patient channel number (0-7) for ADC Ground,

P is electrode number (0-15) for ADC Positive input,

N " " " Negative "

Function: To monitor the electrode voltage across a particular patient channel, the ADC input terminal connections are configured across that channel only. ADC data conversions are initiated at the beginning of every 58 usec. period with the result of the previous period made available immediately upon entry to the interrupt service routine in the DCU. Voltage monitoring may continue for the duration of stimulation. This command may be inserted into any control sequence before the EDC. Due to contact bounce of switching relays, valid data are not available for about 20 msec.

CAUTION: Ambiguous results will be obtained unless the following conventions are followed:

If M = desired patient channel number for voltage monitoring,

then

G = M (0-7)

P = 2M and N = 2M+1 (0-15)

or

P = 2M+1 and N = 2M (0-15)

Impedance Monitoring -

Control Word: AXXI

where I = 0 to exit impedance mode

I = 1 to enter impedance mode.

Function: The impedance mode is a unique mode of operation that allows the measurement of the impedance between any two patient electrodes. The electrodes need not be in the same patient channel. Functionally, the impedance mode allows the programmer to direct the current stimulation from stimulator channel 0 to the electrodes to which the positive and negative inputs of the ADC are connected.

Therefore, to measure the impedance between electrodes Y and Z (0-15), the command sequence is:

Patient Disconnect FXXX

Delay for relay bounce Programmed Delay

Configure ADC for: 9YZ

G = 0, P = Y and N = Z

Note: ADC ground is connected to the floating ground of stimulator channel 0.

Enter Impedance Mode AXX1

Patient Connect EXIX

Delay for relay bounce with multiple EDC's 8008

in order for patient to remain connected

Begin output of stimulus current (***), EOC

on channel 0

Read voltage values during interrupt

processing at beginning of each 50 usec. period

Repeat output and measure cycle 0***, EOC

Complete measurement	
Disconnect Patient	FXXX
Delay for relay bounce	Programmed Delay
Exit Impedance Mode	AXX0

Automated Functional Checkout Routines

Utilizing the various stimulation and monitoring features of the interface, numerous options exist for automated interface checkout and calibration with known resistances in place of the patient. These routines will be specified later.

PATIENT ELECTRODE CONNECTION AND SELECTION

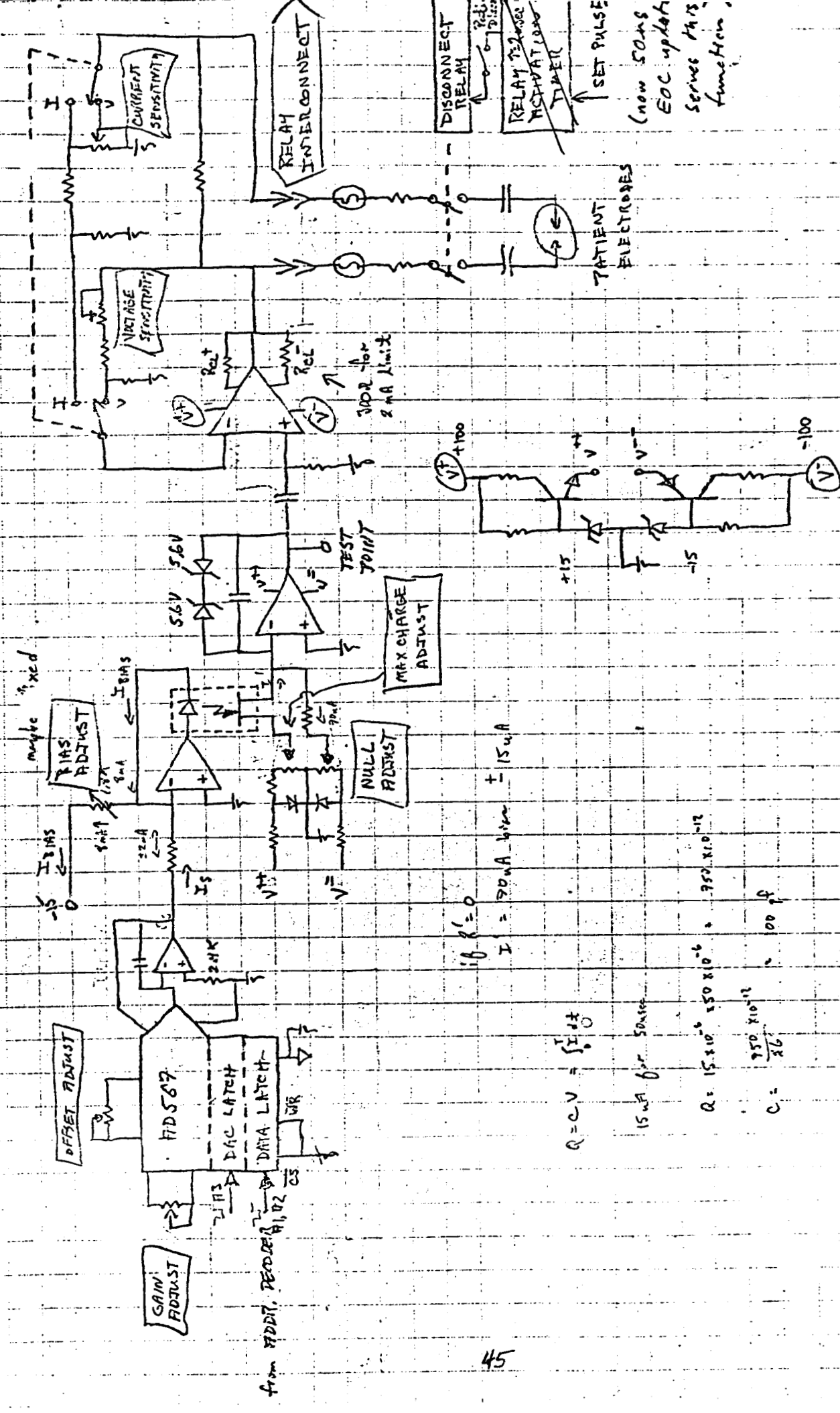
The RTI Patient Interface design departs from the UCSF Interface with regard to the selection of patient electrode configurations. The four channel UCSF system employs a relay matrix which allows complete versatility of electrode configuration under program control. However, as additional channels are added, the switching matrix size rapidly expands to cumbersome limits. For example, to provide full flexibility for an eight channel system would require 256 switching relays, as compared to the four channel system with only 16 relays. Excessive costs and circuit packaging problems make the relay matrix approach unattractive for an eight channel system. Considering that present encoding designs of stimulator systems do not require the ability to change electrode configurations during stimulation, a different electrode selection scheme has been adopted for the RTI design.

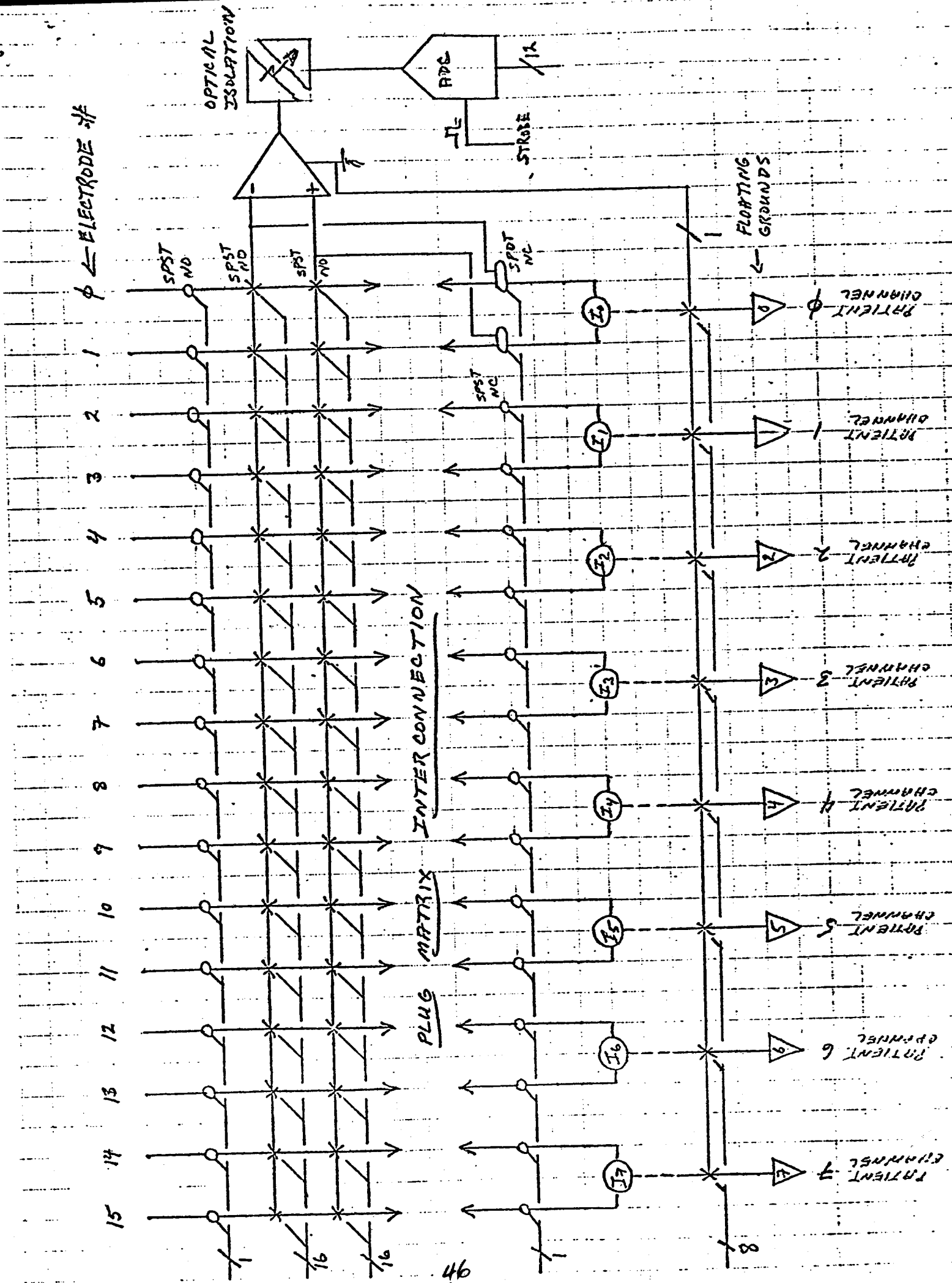
Essentially, a "poor/practical man's" switching matrix is utilized. This consists of a female, panel-mounted, multi-pin connector (miniature Blue Ribbon specifically) which has on one side the outputs from the current stimulators and on the other side the lines to the patient electrode disconnect relays. Electrode configurations are easily selected by plugging in a mating male connector, whose pins have been appropriately jumpered for the required interconnections. Rapid changes of electrode configurations are achieved by simply changing pre-wired jumper plugs. Extra pins on the jumper plugs may be wired so that the computer may verify that the appropriate plug is installed for the present protocol. The jumper plugs make attractive modules when standard cable hoods are installed on the male plugs. Jumper plugs are identified by number.

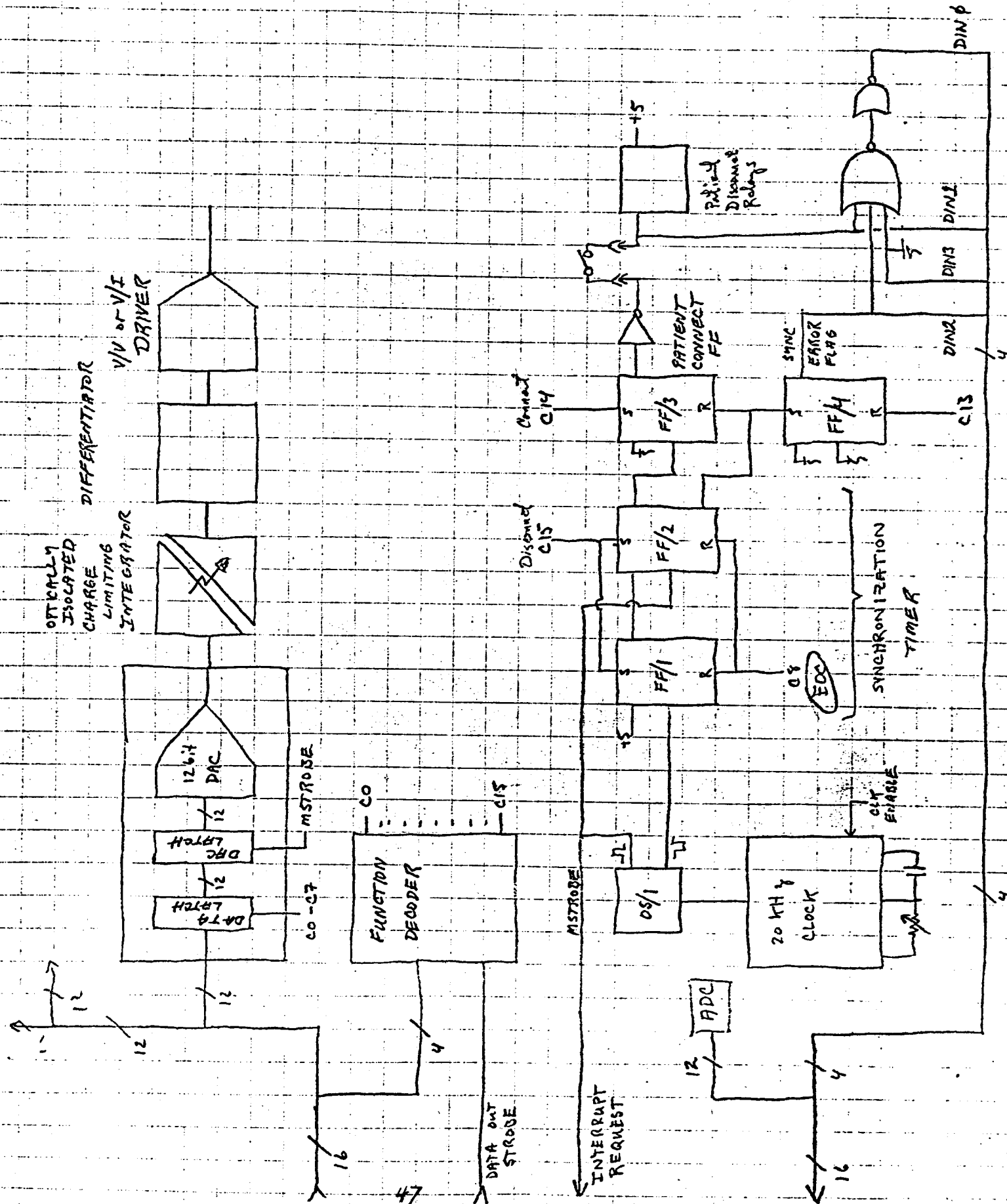
The impedance testing feature of the interface has been constructed so that full flexibility of electrode interconnections is available for impedance measurements under program control, regardless of the installed

jumper configuration. This enables spot checking of impedances between any two electrodes during patient testing.

Should program control of interconnections be required at a later time, an externally-mounted switching circuit could be built and used instead of the prewired jumper plug.







Appendix 2

Notes on Software Development for the Block-Diagram Compiler

Contents:

Structure of Executive Header for Block-Diagram Compiler	49
Functions of Blocks for Block-Diagram Compiler	51
Menus for the "DESIGN" Program	52
Structure of Block Header for Block-Diagram Compiler	54

STRUCTURE OF EXECUTIVE HEADER FOR BLOCK-DIAGRAM COMPILER

3/14/84

SFREQ = sampling frequency;
INB = number of global blocks in the system;
INOUT = number of outputs to be written to the disk

executive first asks for the design #:

ACCEPT 'ENTER DESIGN # ',IDSN

and then IDSN is used to open file DESIGNXXX (using program GENNAME), to read in the headers;

executive then asks for the source of input data, and verifys that the sampling rates are the same; if not the sampling rate of the input is converted to the sampling rate of the simulated system using calls to INTERPOLATE and DOWNSAMPLE;

once the input is specified (and its sampling rate adjusted, if necessary), the executive processes data in 256-word blocks for fast reads and writes to contiguous files on the disk;

a system is simulated by multiple passes through the blocks, where, in each pass, the executive asks if the input(s) to the block have been computed; if so, asks if the output(s) have been computed. If both inputs and outputs have been computed, the executive goes to the next block and asks the same questions. If the input has been computed and the output has not been computed, the output is computed. Finally, if the input has not been computed, control again goes to the next block in the chain. Multiple passes through the network assures computation of all inputs and outputs of all blocks for physically-realizable systems.

once all computations have been completed, the program loops back and asks for another design #, input; etc.

The "modify parameters" program also reads in DESIGNXXX, and asks the user which blocks are to be modified (this can be substitution of another function or changes in the parameters, where the parameters are presented in a menu display so that only the desired subset has to be modified)

the total set of programs will then consist of the following:

CPEXEC -- executive program for bringing the following programs in memory via overlays and virtual overlays;
SAMPLE -- sample speech and other data with the A/D converter, and store these data on the disk in contiguous files with identifying headers;

DESIGN -- design a signal-processing system, where feedback is given on the topology of the network and the attributes of each block, and facilities are provided for correcting errors and revising the design;

MODIFY -- see above;

EXECUTE -- executive program for simulating the signal-processing system on a "once-per-clock-tick" basis; see above for details;

SHOWNTELL -- display outputs of the signal-processing system on the RETRO-Graphics display, or over the D/A converter;

ASNELEC -- assign electrodes to receive data from output files of the signal-processing system, and transform these data into the format for control of the hardware interface between the Eclipse and electrodes;

TEST -- send data out to the electrodes from the file prepared by program ASNELEC; also provide ways to make impedance measurements and to verify that the proper electrode-selection plug is in place for the present test and patient

a good way to provide communication between these programs is via CHAINS so that they do not have to be organized as overlays; in this way, each program can be called as a stand-alone save file.

FUNCTIONS OF BLOCKS FOR BLOCK-DIAGRAM COMPILER

3/14/84

<u>number</u>	<u>function</u>
1	filter (specify filter type; etc.)
2	summer (specify # of inputs; data type -- integer, real or complex)
3	inverter (specify data type)
4	multiplier (specify data type)
5	divider (specify data type)
5.5	window (specify Hanning, Hamming, or extended cosine bell; and window length)
6	FFT analyzer (specify # points; computation of outputs; etc.)
7	LPC analyzer (specify # of coefficients; frequency transformation of output; etc.)
8	rectifier (full-wave or half-wave)
9	pitch extractors (specify cepstral, non-linear wave follower; Gold-Rabiner; Tucker-Bates; etc., and the appropriate parameters for each; format of output: pulse train or level)
9.5	formant trackers (specify type; analysis interval; etc.)
10	compressors (specify type and parameters -- look at Mark White's paper for classes)
11	zero-crossing counter (counter interval; dead zone)
12	level detector (give threshold for a .TRUE. output)
13	one shot (give level for triggering; hysteresis; pulse duration; also provide option for biphasic pulse generation, where each phase is separately specified)
14	switch (closed if logic input is .TRUE. and open if logic input is .FALSE.)
14.5	peak picker (specify analysis interval)
15	flip-flop (specify initial state)
16	other rules to be added

NOTE: all functions are stored in signal-processing library so that only the functions required to implement a given design will be called into core.

MENUS FOR THE "DESIGN" PROGRAM

3/30/84

Two screens are presented to allow the user to select functions for blocks in the block-diagram compiler. The functions now incorporated are a superset of the functions listed on the previous page and provide the tools to specify many (if not all) reasonable designs of speech processors for auditory prostheses. The layouts of screens 1 and 2 are indicated below:

Screen 1

ENTER ONE OF THE FOLLOWING OPTIONS FOR THE FUNCTION OF BLOCK N:

<u>MODULE CATEGORY</u>	<u>OPTION</u>	<u>FUNCTION</u>
DSP:	1 =	FILTER
	2 =	FFT ANALYZER
	3 =	CEPSTRUM ANALYZER
	4 =	WINDOW
SPEECH ANALYSIS:	5 =	LPC ANALYZER
	6 =	FORMANT TRACKER
	7 =	PITCH EXTRACTOR
SIGNAL SOURCE:	8 =	NOISE GENERATOR
	9 =	SIN/COS GENERATOR
	10 =	PULSE-TRAIN GENERATOR
MATH OPERATIONS:	11 =	DISK FILE
	12 =	SUMMER
	13 =	MULTIPLIER/INVERTER
	14 =	DIVIDER
	15 =	LOGARITHMIC CALCULATOR
OTHER:	16 =	INTEGRATOR
	17 =	SHOW REMAINING OPTIONS

ENTER OPTION >

Screen 2

ENTER ONE OF THE FOLLOWING OPTIONS FOR THE FUNCTION OF BLOCK N:

<u>MODULE CATEGORY</u>	<u>OPTION</u>	<u>FUNCTION</u>
CIRCUIT FCNS:	18 =	COMPRESSOR
	19 =	ZERO-CROSSING COUNTER
	20 =	PEAK DETECTOR
	21 =	WINDOW COMPARATOR
	22 =	LEVEL COMPARATOR
	23 =	ONE SHOT (MONOSTABLE MULTIVIBRATOR)
	24 =	FLIP-FLOP
	25 =	SWITCH
	26 =	RECTIFIER
	27 =	UNIT DELAY OPERATOR
OTHER:	28 =	READ SUBSYSTEM FOR PRESENT BLOCK FROM ANOTHER DESIGN
	29 =	SELECT A USER-DEFINED RULE
	30 =	IDENTIFY A USER-DEFINED RULE
	31 =	SHOW TOPOLOGY OF PRESENT SYSTEM
	32 =	RETURN TO PREVIOUS SCREEN
	33 =	REVISE A BLOCK
	34 =	EXIT FROM DESIGN PROGRAM

ENTER OPTION >

Note: The unit delay operator is required for specification of feedback loops within the network.

STRUCTURE OF BLOCK HEADER FOR BLOCK-DIAGRAM COMPILER

3/14/84

IBIL = block length for integer values;
IBFL = block length for floating-point values;
IBCL = block length for complex values;
IFUNC = block function (e.g., = 1 for filter; = 2 for summer; = 3 for inverter; = 4 for multiplier; = 5 for divider; etc.)
ININ = number of inputs;
IN1 = input 1 (= 0 for raw input from disk; = block #/output #, in the two bytes, for intermediate inputs);
.
.
INN = input N;
ICN1 = flag for computation of input 1 (= 0 if this input has not been computed and = 1 if this input has been computed, and automatically set to 1 if input # is 0);
.
.
ICNN = flag for computation of input N;
INOUT = number of outputs
IC01 = flag for computation of output 1 (= 0 if this output has been computed and = 1 if not);
.
.
ICON = flag for computation of output N;
IW01 = flag for writing output 1 to disk (= 0 for no write; = 1 for write);
.
.
IWON = flag for writing output N to disk;
IIPN = number of integer parameters for this function block;
IPARAM1 = integer parameter 1 of function block;
.
.
IPARAMN = integer parameter N of function block;
IIWORDS = number of storage locations reserved for working array of integer values for function block;
IARAY = integer array of dimension IIWORDS;

IFPN = number of floating-point parameters for this function block;
FPARAM1 = floating-point parameter 1 of function block;
.
.
FPARAMN = floating-point parameter N of function block;
IFWORDS = number of storage locations reserved for working array of floating-point values for function block;
FARAY = floating-point array of dimension IFWORDS;
